Low-leakage-current AlGaN/GaN HEMTs on Si substrates with partially Mg-doped GaN buffer layer by metal organic chemical vapor deposition

Li Ming(黎 明)†, Wang Yong(王 勇), Wong Kai-Ming(王凯明), and Lau Kei-May(刘纪美)

Department of Electronic and Computer Engineering, Hong Kong University of Science and Technology, Kowloon, Hong Kong, China

(Received 23 August 2013; revised manuscript received 17 September 2013; published online 24 January 2014)

High-performance low-leakage-current AlGaN/GaN high electron mobility transistors (HEMTs) on silicon (111) substrates grown by metal organic chemical vapor deposition (MOCVD) with a novel partially Magnesium (Mg)-doped GaN buffer scheme have been fabricated successfully. The growth and DC results were compared between Mg-doped GaN buffer layer and a unintentionally one. A 1-μm gate-length transistor with Mg-doped buffer layer exhibited an OFF-state drain leakage current of 8.3×10^{-8} A/mm, to our best knowledge, which is the lowest value reported for MOCVD-grown AlGaN/GaN HEMTs on Si featuring the same dimension and structure. The RF characteristics of 0.25-μm gate length T-shaped gate HEMTs were also investigated.

Keywords: AlGaN/GaN HEMTs, low-leakage current, metal organic chemical vapor deposition, Mg-doped buffer layer

PACS: 84.30.Jc, 85.30.–z, 85.30.Tv **DOI:** 10.1088/1674-1056/23/3/038403

1. Introduction

AlGaN/GaN HEMTs are excellent candidates for power electronics and radio frequency (RF) devices due to their superior properties in high-power, high frequency and high-temperature applications.[1–5] Although sapphire and SiC are commonly used substrates for the growth of AlGaN/GaN HEMTs, silicon is emerging as a promising alternative because of its low cost, large size, as well as its potential for integration with advanced Si electronics. However, the growth of high quality GaN HEMTs on Si is more challenging than that on sapphire or SiC because of the larger mismatches in lattice and thermal expansion coefficient, resulting in a higher density of dislocations and cracks. Moreover, during the growth of GaN films on Si substrates, the auto-doping of silicon from the substrate into the GaN buffer layers may occur at temperatures over 1000 °C, leading to a low resistivity buffer layer and large buffer leakage current. Those issues may cause a low breakdown voltage, which is undesirable for power device operation.

To increase GaN HEMTs' breakdown voltage, many groups have chosen to grow a fairly thick buffer with multiple interlayers for strain management [6]. However, it is difficult to avoid a high density of dislocations and cracks if the buffer layer is too thick. In this study, the doping compensation was utilized to increase the resistivity of the unintentionally doped GaN buffer layer and reduce the buffer leakage current.

A high-resistivity GaN buffer layer grown on a sapphire substrate has been achieved by compensating the donors with acceptor states including Fe-doped, C-doped, and so on,[7–9] the OFF-state breakdown voltages have increased over 1000 V.[8] However, as another acceptor, the growth technology of Mg-doped buffer layers by MOCVD has lagged behind since the Mg-doped buffer layers have been successfully demonstrated,[10,11] and the details of AlGaN/GaN HEMT with Mg-doped buffer layers by MOCVD need to be further explored.

Therefore, in this work, we have used a buffer layer less than 2 μm thick, with a partially Mg-doped 1.0 μm GaN portion to increase the buffer resistivity. The DC and RF characteristics will be compared between the samples with Mg-doping and without Mg-doping.

2. Experiment

The $Al_{0.25}GaN$/GaN HEMTs were grown on 2-inch Si (111) substrates by low-pressure MOCVD in an Aixtron 2000HT system. The Si substrates were high resistivity (> 3000 Ω·cm) and 280 μm thick. Trimethylgallium (TMGa), trimethylaluminum (TMAl), trimethylindim (TMIn) and ammonia (NH_3) were used as the Ga, Al, In and N precursors, respectively. Biscyclopentadienyl magnesium (Cp_2Mg) was used as the p-type dopant, while silane (SiH_4) was used as the n-type dopant, H_2 or N_2 served as the carrier gas. The as-grown epi-layer structure of the AlGaN/GaN HEMTs on Si is shown in Fig. 1.

Prior to the growth, the substrates were heated up to 1190 °C for 10 minutes in an H_2 atmosphere to remove the native oxide. Then, a 40 nm-thick AlN nucleation layer was deposited at 1150 °C, followed by a SiN_x mask layer growth at 1160 °C [12]. This SiN_x mask did not cover the AlN surface

†Corresponding author. E-mail: eeliming@sina.com

© 2014 Chinese Physical Society and IOP Publishing Ltd

completely. The partial coverage served the purpose of enhancing lateral growth of GaN with better crystalline quality. A 0.8 μm-thick undoped GaN layer was grown on the partially exposed AlN nucleation layer with a SiN_x *in situ* mask at 1170 °C. After that, stacked AlGaN/AlN interlayers were grown on top to further reduce the tensile stress, with a growth temperature of 950 °C for the AlN layer and 1150 °C for the AlGaN layer. Subsequently, a continuous 1 μm-thick GaN buffer (consisting of an 875 nm-thick undoped portion on top of a 125 nm-thick Mg^{2+} doped lower region) was grown at 1170 °C. Finally the barrier structure was grown, including 1 nm AlN spacer and 20 nm $Al_{0.25}Ga_{0.75}N$ barrier layer.

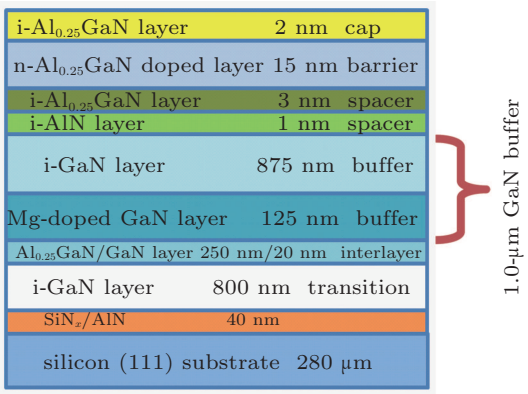


Fig. 1. (color online) Schematic of AlGaN/GaN HEMT buffer layer structure on Si substrates.

The surface morphology of buffer layers with sample A (with Mg-doped) and sample B (without Mg-doping) were characterized by an atomic force microscope (AFM). From figure 2, the surface root mean square (RMS) roughness of both samples A and B are 0.8 nm, which indicates that the GaN buffer layer still maintains quite a smooth surface morphology after the introduction of Mg dopant.

Figure 3 plots the SIMS curves of the Mg dopant profiles in both the referential samples A and B as functions of depth from the surface. A clear Mg peak can be found in Fig. 3(a). In addition, the oxygen content in the buffer with Mg-doping (Fig. 2(a)) is lower than that in other buffers without Mg-doping (Fig. 2(b)), which may create a lower buffer leakage current and better device performance.[13]

The pinch-off voltage V_{th} and AlGaN barrier layer thickness d of both the samples A and B were characterized by the mercury-probe capacitance–voltage (C–V) analyzer. As shown in table 1, sample A shows almost the same mobility and channel sheet resistance (R_s) compared with sample B, which means that Mg-doping in the GaN buffer layer did not introduce too much impurity scattering and reduced the mobility in the 2DEG.

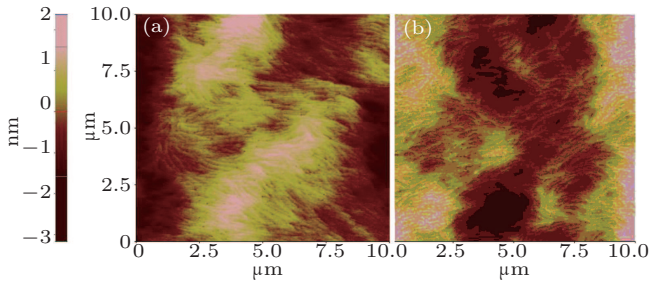


Fig. 2. (color online) AFM images of sample A, partially Mg-doped: RMS = 0.8 nm (a) and sample B without Mg-doping: RMS = 0.8 nm (b).

Table 1. Comparison of mercury-probe C–V and 2DEG profiles of samples A and B.

Samples	C–V results		Hall results		
	V_{th}/V	d/nm	Mobility /(cm^2/V·S)	R_s/(Ω/□)	N_s/cm^{-2}
with Mg-doped	−4.0	22.5	1230	298	-1.71×10^{13}
without Mg-doped	−3.9	21.8	1260	280	-1.77×10^{13}

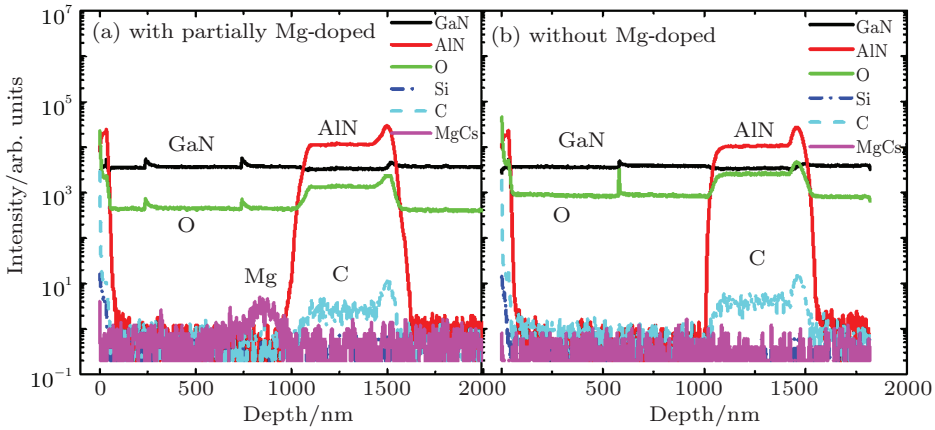


Fig. 3. (color online) SIMS measurements of the Mg of samples A (a) and B (b).

A quite standard HEMT process has been done with sample A and sample B for comparison. The gate length of the devices was 1 μm, with 1 μm gate–source and 1 μm gate–drain spacing. No additional passivation processes or plasma treatments were utilized in this study. The 0.25 μm T-shaped gate device was also done by a simplified trench fabrication process. The 100 nm-thick Si_3N_4 was deposited on the epitaxial layers by plasma-enhanced chemical vapor deposition

(PECVD). The gate was defined by a JEOL JBX-6300 e-beam lithography system with ZEP520A photoresist. The gate pattern was then transferred to the Si_3N_4 by dry etching. The inset of figure 7 shows a cross-sectional SEM photograph of the HEMT with a 250 nm T-shaped gate and an 800 nm-wide head.

3. Results and discussion

The buffer leakage current was assessed by the structure in Fig. 4, where the source drain was isolated by plasma etching. The leakage current of sample A is almost three orders of magnitude lower than sample B with the voltage between drain and source $V_{DS} = 0$ V–10 V and the distance between drain and source $L_{DS} = 10$ μm, which indicates the higher resistivity of the Mg-doped buffer layer than that without Mg-doping.

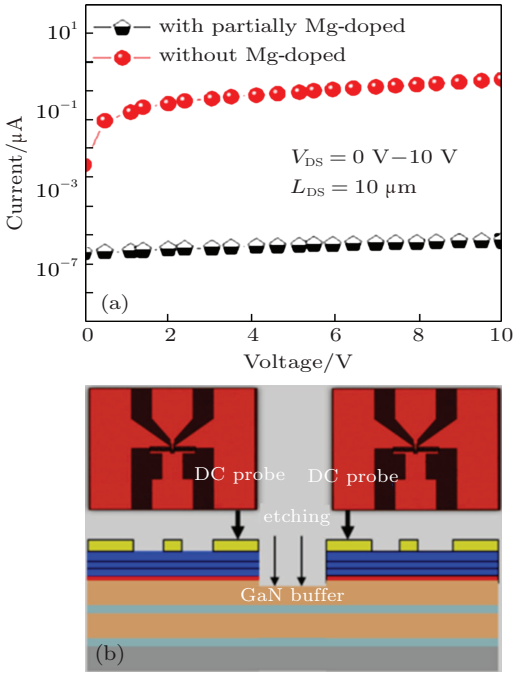


Fig. 4. (color online) (a) Buffer leakage current of AlGaN/GaN HEMT on Si substrates. (b) The testing pad diagram.

Figure 5 shows a typical current–voltage (I–V) and transfer characteristics of the AlGaN/GaN HEMTs with a Mg-doped buffer layer and without a Mg-doped buffer layer. The maximum drain current of HEMT with a Mg-doped buffer layer was 1.1 A/mm at $V_{GS} = 2$ V and $V_{DS} = 10$ V. The maximum extrinsic transconductance was about 300 mS/mm at $V_{GS} = -0.4$ V and $V_{DS} = 10$ V, the device threshold voltage was around −2.3 V. A recorded OFF-state drain leakage current of 8.3×10^{-8} A/mm (at $V_{GS} = -8$ V and $V_{DS} = 10$ V) have also been observed compared with those featuring the same dimensions and structure [11–14]. An ON/OFF current ratio up to 1.33×10^7 was also obtained. Figure 6(a) shows the measured gate leakage current $I_{GS} = 7.9 \times 10^{-6}$ A/mm (with partial Mg-doping) and 6.4×10^{-4} A/mm (without Mg-doping) at $V_{GS} = -35$ V, respectively, which confirmed that the drain-to-source leakage through the buffer layer was dramatically reduced.

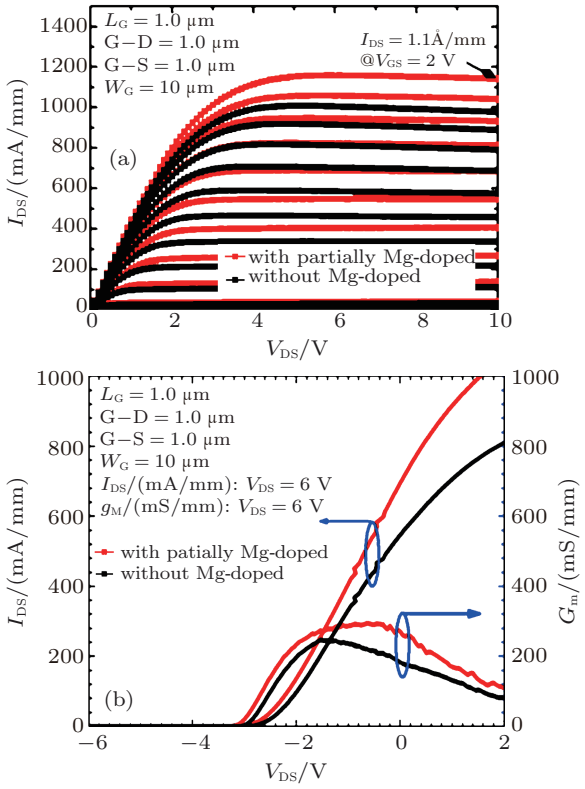


Fig. 5. (color online) Typical I–V and transfer characteristics of a $L_G = 1.0$ μm HEMT (sample A), L_G and W_G mean gate length and gate width, respectively, G–D and G–G mean the distance between gate and drain and the distance between gate and source, respectively, g_M is transconductance.

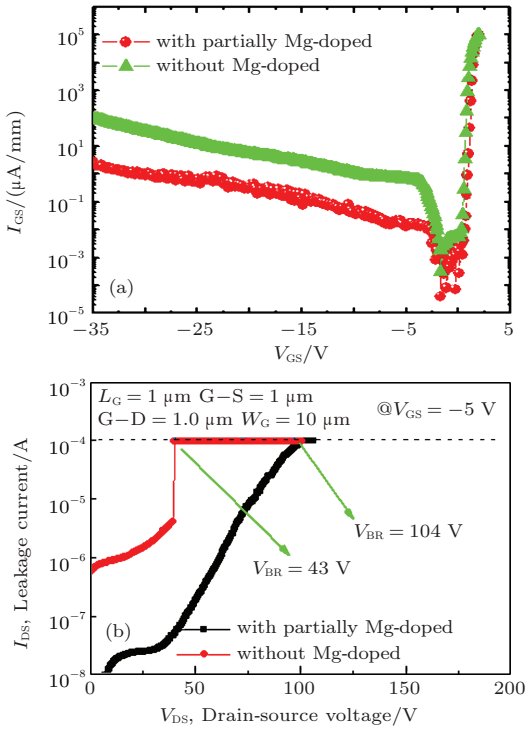


Fig. 6. (color online) (a) OFF-state breakdown characteristics of the fabricated AlGaN/GaN HEMTs with a Mg^{2+} doping GaN buffer on Si substrates OFF-state breakdown voltages (V_{BR}). (b) Measured gate leakage current as a function of gate bias.

In addition, as shown in Fig. 6(b), the OFF-state breakdown voltage of GaN-based HEMT (V_{BR} = 104 V) with a partial Mg-doped buffer layer could be increased dramatically compared with the standard HEMT without a Mg-doped buffer (V_{BR} = 43 V).

The DC characteristics of the devices with a Mg-doped buffer layer are rather comparable to the state of the art of GaN HEMTs that have been reported during the last few years [15–20]. The OFF-state drain leakage current of the device was successfully reduced to 8.3×10^{-8} A/mm, to our best knowledge, which is the lowest with the same dimensions and structure,[11–14] confirms that the partially Mg-doped GaN buffer layer is an effective way to reduce the leakage current of transistors.

The RF characteristics of both samples A and B were also compared using cascade microtech probes and an HP8722 network analyzer from 0.1 GHz to 39.1 GHz. As presented in Fig. 7, 0.25-μm gate-length AlGaN/GaN HEMT with a Mg-doped buffer layer exhibits f_T = 31.3 GHz (f_T means the current-gain cutoff frequency) and f_{max} = 22.3 GHz (f_{max} means the maximum available gain) while the standard HEMT without Mg-doping shows f_T = 40 GHz and f_{max} = 26 GHz, at the optimum bias condition of $V_{GS} = -1.0$ V and V_{DS} = 10 V. Although the HEMT with a Mg-doped buffer layer achieves comparable extrinsic G_m, 21% lower f_T and 14% lower f_{max} are observed. Gate-to-source capacitance C_{gs} and gate-to-drain capacitance C_{gd} are extracted from S-parameters at V_{GS} with maximum G_m. The HEMT with a Mg-doped buffer layer achieves C_{gs} = 0.3 pF/mm and C_{gd} = 0.052 pF/mm, much higher than those of the standard HEMT (C_{gs} = 0.25 pF/mm, C_{gd} = 0.045 pF/mm). The drastically increased C_{gs} and C_{gd} result in a lower ratio of transconductance-to-gate capacitance, leading to significantly decreased RF performance. These results mean that the Mg-doped buffer layer could bring some disadvantage to the RF performance as the increased parasitic capacitance scheme of the buffer layer. Further explorations are necessary to fully reveal the mechanism of the Mg-doped buffer layer.

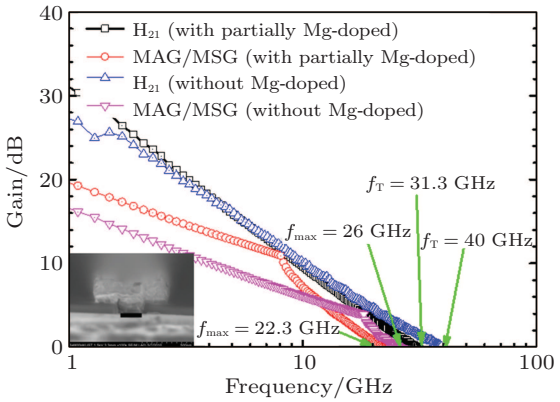


Fig. 7. (color online) Small signal RF characteristics of 0.25 μm devices.

Table 2 shows the comparison of different AlGaN/GaN HEMT performances, which were grown by MBE or MOCVD on sapphire or Si substrates with similar dimensions of HEMTs. The DC performance of HEMTs with Mg-doped buffer layers is favored compared with that of HEMT technology with multiple interlayers or C- and Fe-doping. These results are very encouraging toward integrating high speed and high frequency power devices on Si platforms by MOCVD.

Table 2. Comparison of AlGaN/GaN HEMT performance. L_g, W_g and L_{gd} are the gate length, the gate width and the distance between gate and drain, respectively.

Structures	Size	Breakdown voltages	Approaches	Year	Ref.
AlGaN/GaN HEMT, on patterned Si	$L_g/W_g/L_{gd} = 1/100/2$ μm	V_{bk} = 50 V	patterned substrate	2005	[15]
AlGaN/GaN HEMT, on grooved sapphire	$L_g/W_g/L_{gd} = 1/100/1$ μm	V_{bk} = 74 V	thick buffer layer	2005	[16]
AlGaN/GaN HEMT, on sapphire	$L_g/W_g/L_{gd} = 0.7/150/1$ μm	V_{bk} = 90 V	thick GaN cap layer	2004	[17]
AlGaN/GaN/InGaN/GaN	$L_g/W_g/L_{gd} = 1/10/1$ μm	$V_{bk} > 60$ V	new structure	2007	[18]
AlGaN/GaN HEMT, on sapphire	$L_g/W_g/L_{gd} = 1/10/3$ μm	V_{bk} = 95 V	low density drain (LDD)	2007	[19]
AlGaN/GaN HEMT, on Si	$L_g/W_g/L_{gd} = 1/10/2$ μm	V_{bk} = 90 V	fluorine ion implantation	2011	[20]
AlGaN/GaN HEMT, on Si	$L_g/W_g/L_{gd} = 1/10/1$ μm	V_{bk} = 104 V	Mg-doped buffer layer	2012	this paper

4. Conclusion

In conclusion, high-performance low-leakage-current AlGaN/GaN HEMTs on silicon (111) substrates grown by MOCVD have been fabricated successfully. A partially Mg-doped GaN buffer has been introduced to increase the buffer resistivity and reduce the leakage current. A 1 μm gate-length transistor exhibited a recorded OFF-state drain leakage current of 8.3×10^{-8} A/mm and a high ON/OFF current ratio up to 1.33×10^{7} (V_{GS} from −8 V to 2 V and V_{DS} = 10 V). The results show that MOCVD-grown AlGaN/GaN HEMTs on Si with a Mg-doped buffer scheme are a promising prospect for integrating high speed and high frequency power devices on Si platforms.

References

[1] Uemoto Y, Shibata D, Yanagihara M, Ishida H, Matsuo H, Nagai S, Batta N, Li M, Ueda T, Tanaka T and Ueda D 2007 *IEDM Tech. Digest.* 861

[2] Wu Y F, Saxler A, Moore M, Smith R P, Sheppard S, Chavarkar P M, Wisleder T, Mishra U K and Parikh P 2004 *IEEE Electron Device Lett.* **25** 117

[3] Vertiatchikh A V and Eastman L F 2003 *IEEE Electron Device Lett.* **24** 535
[4] Shi L, Feng S W, Guo C S, Zhu H and Wan N 2013 *Chin. Phys. B* **22** 027201
[5] Meneghesso G, Verzellesi G, Danesin F, Rampazzo F, Zanon F, Tazzoli A, Meneghini M and Zanoni E 2008 *IEEE Trans. Device Mater. Rel.* **8** 332
[6] Nariaki I, Jiang L, Kazuo K, Shuusuke K, Kazama T, Kokawa T, Sato Y, Iwami M, Nomura T and Masuda M 2008 *High-Density Multi-Fiber Connectors for Optical Interconnection, Furukawa Review* **34** 17
[7] Young C C, Ho Y C, Boris P, Michael G S and Lester F E 2006 *IEEE Electron Device Lett.* **53** 2926
[8] Choi Y, Shi J, Pophristic M, Spencer M and Eastman L 2007 *J. Vac. Sci. Technol. A* **25** 1836
[9] Cordiera Y, Azizea M, Barona N, Bougrioua Z, Chenot S, Tottereau O, Massies J and Gibart P 2008 *J. Cryst. Growth* **310** 948
[10] Pan C J and Chi G C 1999 *Solid State Electron.* **43** 621
[11] Yang Y J, Yen J L, Yang F S and Lin C Y 2000 *Jpn. J. Appl. Phys.* **39** 390
[12] Yu N, Wang Y, Wang H, Ng K and Lau K 2009 *Sci. China Ser. E* **52** 2758
[13] Pearton S J, Abernathy C R, Thaler G T, Frazier R, Ren F, Hebard A F, Park Y D, Norton D P, Tang W, Stavola M, Zavada J M and Wilson R G 2003 *Physica B* **39** 340
[14] Oku T, Kamo Y and Totsuka M 2008 *Thin Solid Films* **516** 545
[15] Jia S, Dikme Y, Wang D L, Chen K J, Lau K M and Heuken M 2005 *IEEE Electron Device Lett.* **26** 130
[16] Feng Z H, Cai S J, Chen K J and Lau K M 2005 *IEEE Electron Device Lett.* **26** 870
[17] Shen L, Coffie R, Buttari D, Heikman S, Chakraborty A, Chini A, Keller S, DenBaars S P and Mishra U K 2004 *IEEE Electron Device Lett.* **25** 1
[18] Liu J, Zhou Y G, Zhu J, Lau K M and Chen K J 2006 *Phys. Stat. Sol. (c)* **3** 2312
[19] Song D, Liu J, Cheng Z Q, Tang C W, Lau K M and Chen K J 2007 *IEEE Electron Device Lett.* **28** 189
[20] Wang M 2011 *IEEE Trans. Electron Dev.* **58** 460